KSME

Springer

Journal of Mechanical Science and Technology 36 (3) 2022

Original Article
DOI 10.1007/s12206-022-0236-1

Keywords:
· Adaptive control
· Bounded inputs
· Force/position control
· Generalized saturation functions
· Robot manipulator

Correspondence to:
Marco Mendoza-Gutiérrez
marco.mendoza@uaslp.mx

Citation:
Rojas-García, L., Bonilla-Gutiérrez, I., Mendoza-Gutiérrez, M., Chávez-Olivares, C. (2022). Adaptive force/position control of robot manipulators with bounded inputs. Journal of Mechanical Science and Technology 36 (3) (2022) 1497~1509. http://doi.org/10.1007/s12206-022-0236-1

Received May 18th, 2021
Revised October 30th, 2021
Accepted November 15th, 2021

† Recommended by Editor
Ja Choon Koo

Adaptive force/position control of robot manipulators with bounded inputs

Lina Rojas-García[1], Isela Bonilla-Gutiérrez[1], Marco Mendoza-Gutiérrez[1] and César Chávez-Olivares[2]

[1]Faculty of Sciences, Autonomous University of San Luis Potosí, San Luis Potosí 78295, Mexico, [2]Robotics Engineering Department, Autonomous University of Aguascalientes, Aguascalientes 20340, Mexico

Abstract In various automated industrial, medical, or service applications using robotic systems it is required to regulate both robot movement and contact force. In order to address this control problem, this paper presents a force/position control structure that has two characteristics that are very relevant in robot-environment interaction tasks. First, the structure of the controller is based on the use of generalized saturation functions, and this makes it possible to ensure that the robot actuators operate within a safe region without exceeding their torque limits. On the other hand, an adaptable term is included within the structure that allows to compensate for parametric uncertainty related to gravitational forces and the stiffness of the environment on which the robot operates. The validity and correct performance of the proposed control structure is based on a rigorous stability analysis, as well as numerical simulations using a three-degree-of-freedom robot manipulator.

1. Introduction

Day by day, robotic systems are used in increasingly complex tasks within diverse areas ranging from industrial or research applications to rehabilitation therapy processes [1, 2]. When such tasks require physical interaction between a robot and its environment, it is necessary to ensure a safe interaction between them for the task to be performed successfully [3, 4]. Now, during these tasks of robot-environment interaction, the contact forces can cause damage to both and therefore these forces must be regulated. In order to ensure the safety of both the robotic system and the environment in interaction tasks, different research groups have proposed very diverse solutions [5-7]. In general, interaction control algorithms can be classified into explicit and implicit force controllers [8]. In explicit force control, the measured contact forces/torques are compared to the predefined desired values, thus achieving an appropriate interaction when the robot applies a specific force/torque level over environment or vice versa. On the other hand, for implicit force control algorithms it is not possible to set desired force values, but from the generated contact forces it is possible to modify the desired movement of the robot without specifying a level of force required to interact appropriately and thus indirectly regulate the force.

In many cases, both implicit and explicit force control strategies often have structures based on the robot model in order to compensate for various dynamic effects [9]. In the case of regulation (position control), the main effect to compensate is gravitational force/torque, however the parameters associated with this effect are not always known with precision and, therefore, adaptive schemes or intelligent controllers are often used [10, 11]. On the other hand, the modeling of the environment depends on parameters such as mass, damping or stiffness, which are also often unknown with precision and can vary depending on the material of the object or surface with which the robot must interact [12]. Therefore, in this work, it was decided to design a control scheme that can be adapted to the parametric uncertainty of gravitational forces and the stiffness of the environment, in order that it can be implemented in different robot manipula-

tors that interact with unknown environments.

In industrial environments, there are several robotic tasks that require precise control of the contact force, among them we find polishing, deburring, component assembly, etc. These problems are usually addressed from two perspectives: a) improving the mechanical design of the robotic system, or b) improving the control system. From the point of view of mechanical design, a very interesting proposal was recently presented by Azizi [13], where a genetic algorithm is used to find optimal parameters of gimbal joints and it was observed that the robot's manipulability improves, because the amount of force delivered by a gimbal equipped robot is greater than the force delivered by a robot that uses revolute joints. On the other hand, from the control perspective and to achieve a stable closed loop response in this type of applications, Chávez-Olivares et al. propose a family of explicit force controllers that are theoretically supported by a stability analysis in the sense of Lyapunov [14]. However, the control algorithms derived from the above proposal do not simultaneously regulate position (motion) and force, nor do they consider that the robot actuators cannot deliver any torque value. This second perspective is what we address and improve in this work where we propose a control structure that respects the torque limits of the robot.

Winkler et al. carried out a comparison between implicit and explicit force control algorithms for robot manipulators, and they define the characteristics of interaction tasks suitable for each control structure [15]. As a result of the comparative study, it was found that stiffness control is not suitable for tasks where the robot is in free space and the distance between its end-effector and the contact surface is unknown, while impedance control is not suitable when the robot is in contact with the environment, because the mass component can cause instability. Whereas hybrid or parallel force/position control is suitable when it is required that the interaction forces and end-effector position being simultaneously regulated [16-18]. For example, in Ref. [16] Rani and Kumar propose a hybrid controller for collaborative interaction tasks using a neural network to estimate unmodeled robot dynamics, resulting in correct position and force regulation, however, like most they ignore the torque saturation limits of actuators and consider that the object handled by the robots is rigid and non-deformable. In a very recent work, Gutierrez-Giles et al. propose a scheme for position and force regulation for industrial robots interacting with rigid and soft environments, however, their proposal focuses on systems with closed control architecture and therefore it is a kinematic-type structure that assumes that the robot dynamics is adequately regulated by a standard PID controller [17]. Another alternative is to model a deformable environment as a damping-spring system, in Ref. [18] Huang et al. present an optimal force/position regulation scheme for collaborative robotic tasks and that allows interaction with an object with unknown mass, damping or stiffness, however, it is also a kinematic solution where a PID controller regulates robot dynamics. In addition, these force/position control schemes lack a closed-loop stability analysis to serve as a theoretical basis of validity, so our proposal seeks to address this very common flaw in these types of controllers.

In recent years, several control schemes with bounded actions have been developed, mainly addressing the problems of regulation and tracking in tasks where the robot moves freely [19-22]. However, very few results have been obtained using interaction control schemes that generate bounded actions and the work has focused on implicit force control by proposing stiffness control algorithms [23, 24], but as explained above, these are not appropriate when the robot is in free space and the distance between its end effector and the contact surface is unknown, which is addressed in this document using an explicit force controller. There are also some hybrid force/position controllers such as Refs. [25, 26] that take into account torque constraints in the robotic system. However, the proposed structure in Ref. [25] restricts the gain adjustment to achieve bounded actions, resulting in a decrease in performance or convergence of force/position errors, while the proposed controller in Ref. [26] represents a kinematic solution that regulates the force indirectly and that does not guarantee the stability of the closed-loop equilibrium point. Within this context, our proposal focuses on addressing or solve the following issues:

1. Interaction tasks in which a robot comes into contact with deformable objects whose stiffness is unknown and there is uncertainty regarding the robot's dynamic parameters (particularly in the case of regulation, those associated with gravitational forces/torques).

2. For safe interaction tasks, when the distance between the robot's end effector and the contact surface is unknown, it is important to design explicit force control schemes that generate bounded actions.

3. Design dynamic-type bounded control structures that ensure the stability of the closed-loop equilibrium point and whose gain tuning process does not affect performance to achieve bounded control actions.

Therefore, the proposed force/position control scheme uses generalized saturation functions to ensure that the actuators of the robotic system operate within a safe region (without exceeding their torque limits) and it allows the unrestricted selection of control gains to improve the performance of the controller. Likewise, to compensate for the parametric uncertainty related to gravitational forces and stiffness, the scheme includes an adaptive term within its structure. In addition, the proposed control scheme has a rigorous stability analysis that validates its correct functioning and, as an example, numerical simulation results are presented using a robot manipulator of three degrees of freedom.

2. Preliminaries

2.1 Notation and definitions

In this paper, matrices and vectors are represented as $A \in \mathbb{R}^{n\times m}$ and $y \in \mathbb{R}^n$, respectively, while A_i is the i-th row

vector of matrix A, A_{ji} is the element of matrix A located in the i-th row and the j-th column, and y_i represents the i-th element of vector y. The origin of $\mathbb{R}^n$ is denoted by 0_n and the $n\times n$ identity matrix is represented as I_n. The Euclidean norm of vectors and the induced norm of matrices are denoted by $\|y\|=\sqrt{y^T y}$ and $\|A\|=\sqrt{\lambda_{\max}\{A^T A\}}$, respectively, where $\lambda_{\max}\{A^T A\}$ is the maximum eigenvalue of matrix $A^T A$.

Let $\zeta:\mathbb{R}\mapsto\mathbb{R}$ be a continuously differentiable scalar function and $\varphi:\mathbb{R}\mapsto\mathbb{R}$ be a locally Lipschitz, continuous, scalar function, both vanishing at zero, i.e., $\zeta(0)=\varphi(0)=0$. In addition, ζ' represents the derivative of ζ with respect to its argument, i.e., $\zeta'(\varsigma)=\partial\zeta(\varsigma)/\partial\varsigma$. While the upper right-hand derivative of φ is given by $D^+\varphi(\varsigma)=\limsup_{h\to 0^+}\{[\varphi(\varsigma+h)-\varphi(\varsigma)]/h\}$, $\forall\varsigma\in\mathbb{R}$, thus $\varphi(\varsigma)=\int_0^{\varsigma}D^+\varphi(r)dr$ [27].

Definition 1. A nondecreasing Lipschitz-continuous function $\sigma:\mathbb{R}\to\mathbb{R}$ bounded by $M>0$ is a generalized saturation function (GSF) if

a) $\varsigma\sigma(\varsigma)>0$, $\forall\varsigma\neq 0$.

b) $|\sigma(\varsigma)|\le M,\forall\varsigma\in\mathbb{R}$.

Definition 2. σ is a linear generalized saturation function (LGSF) if $\sigma(\varsigma)=\varsigma$ when $|\varsigma|\le L$, for some $0<L\le M$.

According to Refs. [19, 24], a GSF σ has the following properties for a constant $k>0$:

1) $\lim_{|\varsigma|\to\infty}D^+\sigma(\varsigma)=0$.

2) $\exists\sigma'_M\in(0,\infty):0\le D^+\sigma(\varsigma)\le\sigma'_M$, $\forall\varsigma\in\mathbb{R}$.

3) $\sigma^2(k\varsigma)/[2k\sigma'_M]\le\int_0^{\varsigma}\sigma(kr)dr\le k\sigma'_M\varsigma^2/2$, $\forall\varsigma\in\mathbb{R}$.

4) $\int_0^{\varsigma}\sigma(kr)dr>0$, $\forall\varsigma\neq 0$.

5) $\int_0^{\varsigma}\sigma(kr)dr\to\infty$ as $\varsigma\to\infty$.

6) If σ is strictly increasing, then

a) $\varsigma[\sigma(\varsigma+\eta)-\sigma(\eta)]>0$, $\forall\varsigma\neq 0$, $\forall\eta\in\mathbb{R}$.

b) $\bar{\sigma}(\varsigma)=\sigma(\varsigma+a)-\sigma(a)$ is a strictly increasing GSF, bounded by $\bar{M}=M+|\sigma(a)|$ for any constant $a\in\mathbb{R}$.

7) If σ is a LGSF for (L,M) then, for any continuous function $\nu:\mathbb{R}\mapsto\mathbb{R}$ such that $|\nu(\eta)|<L$, it holds that $\varsigma[\sigma(\varsigma+\nu(\eta))-\sigma(\nu(\eta))]>0$, $\forall\varsigma\neq 0$, $\forall\eta\in\mathbb{R}$.

2.2 Dynamics of robot manipulators

The Euler-Lagrange dynamical equation for robot manipulators of n degrees of freedom is given by

$$H(q)\ddot{q}+C(q,\dot{q})\dot{q}+F\dot{q}+g(q)=\tau-J^T(q)f_e \tag{1}$$

where $q\in\mathbb{R}^n$, $\dot{q}\in\mathbb{R}^n$ and $\ddot{q}\in\mathbb{R}^n$ are the joint position, velocity and acceleration vectors, respectively. $H(q)\in\mathbb{R}^{n\times n}$, $C(q,\dot{q})\in\mathbb{R}^{n\times n}$ and $F\in\mathbb{R}^{n\times n}$ are matrices of inertia, centripetal and Coriolis, and viscous friction, respectively. While $J(q)\in\mathbb{R}^{m\times n}$ represents the analytical Jacobian matrix of the robot. Finally, $g(q)\in\mathbb{R}^n$, $\tau\in\mathbb{R}^n$ and $f_e\in\mathbb{R}^m$ are vectors of gravitational, control and external interaction torques, respectively.

The dynamical model Eq. (1) has the following properties [28]:

Property 1. $H(q)$ and F are positive definite symmetric matrices, even F is diagonal.

Property 2. For robots with only revolute joints, $g(q)$ is bounded on $\mathbb{R}^n$ in such a way that $|g_i(q)|\le B_{gi}$, $\forall q\in\mathbb{R}^n$ and non-negative constants B_{gi}, i = 1, …, n.

Property 3. The vector $g(q)$ can be represented as $g(q,\theta_g)=G(q)\theta_g$, where $G(q)\in\mathbb{R}^{n\times p}$ is a regression matrix and $\theta_g\in\mathbb{R}^p$ is a constant vector of robot parameters.

Property 4. For the gravity vector $g(q,\theta_g)$, let θ_{Ml} be an upper bound so that $|\theta_{gl}|\le\theta_{Ml}$, $\forall l\in\{1,...,p\}$, and let $\theta_M\triangleq(\theta_{M1},...,\theta_{Mp})^T$ and $\Theta\triangleq[-\theta_{M1},\theta_{M1}]\times\cdots\times[-\theta_{Mp},\theta_{Mp}]$. According to Properties 2 and 3, there are $B_{gi}^{\theta_M}>0$ such that $|g_i(y,w)|=|G_i(y)w|\le B_{gi}^{\theta_M}$, $\forall y\in\mathbb{R}^n$ and $\forall w\in\Theta$. In addition, there are non-negative constants such that $|G_{il}(y)|\le B_{Gil}$, $\|G_i(y)\|\le B_{Gi}$ and $\|G(y)\|\le B_G$, $\forall y\in\mathbb{R}^n$, $\forall l\in\{1,...,p\}$, i = 1, …, n.

Property 5. For robots with only revolute joints, there are non-negative constants such that $|J_{ij}^T(y)|\le B_{Jij}$, $\|J_i^T(y)\|\le B_{Ji}$ and $\|J^T(y)\|\le B_J$, $\forall y\in\mathbb{R}^n$, i = 1, …, n, j = 1, …, m.

Assumption 1. For robots with bounded inputs, each element of vector τ is bounded by $T_i>0$, i.e., $|\tau_i|\le T_i$, i = 1, …, n. Assume that

$$\tau_i=T_i\,\mathrm{sat}(u_i/T_i) \tag{2}$$

where sat(·) is the standard saturation function, i.e., $\mathrm{sat}(\varsigma)=\mathrm{sign}(\varsigma)\min\{|\varsigma|,1\}$ and u_i denotes the i-th control signal. In addition, assume that $T_i>B_{gi}$, $\forall i\in\{1,...,n\}$.

By means of the forward kinematics mapping $x=\mathcal{K}(q)$, the dynamical model Eq. (1) can be rewritten in task space as

$$H_x\ddot{x}+C_x\dot{x}+F_x\dot{x}+g_x=f_x-f_e \tag{3}$$

where $\dot{x}=J(q)\dot{q}\in\mathbb{R}^m$ and $\ddot{x}=\dot{J}(q,\dot{q})\dot{q}+\mathrm{J}(q)\ddot{q}\in\mathbb{R}^m$ are the vectors of task-space velocity and acceleration, respectively. f_x is a vector of control forces such that $\tau=J^T(q)f_x$. While $H_x=[J^{-1}(q)]^T H(q)J^{-1}(q)$, $C_x=[[J^{-1}(q)]^T C(q,\dot{q})-H_x\dot{J}(q,\dot{q})]J^{-1}(q)$, $F_x=[J^{-1}(q)]^T FJ^{-1}(q)$ and $g_x=[J^{-1}(q)]^T g(q)$. This model is valid only if the robot is away from kinematic singularities and, when the robot is redundant, the right pseudo-inverse of $J(q)$ can be considered [29].

In order to model the forces of robot-environment interaction, the following assumption is considered:

Assumption 2. The external forces f_e can be represented as a generalized spring

$$f_e = K_e\left[x - x_e\right] \tag{4}$$

where $K_e \in \mathbb{R}^{m\times m}$ is a positive definite diagonal stiffness matrix and $x_e \in \mathbb{R}^m$ is the spring rest position.

The dynamic model Eq. (3) has the following properties [23, 24]:

Property 6. For some constants $\mu_M \geq \mu_m > 0$, $H_x \in \mathbb{R}^{m\times m}$ satisfies $\mu_m I_m \leq H_x \leq \mu_M I_m$.

Property 7. For some constant $k_c \geq 0$, $C_x \in \mathbb{R}^{m\times m}$ satisfies $\left\|C_x\dot{x}\right\| \leq k_c\left\|\dot{x}\right\|^2$, $\forall \dot{x} \in \mathbb{R}^m$.

Property 8. For some constants $f_M \geq f_m > 0$, $F_x \in \mathbb{R}^{m\times m}$ satisfies $f_m I_m \leq F_x \leq f_M I_m$.

Property 9. The matrices C_x and $\dot{H}_x \triangleq dH_x/dt$ satisfy $\dot{x}^T\left[\dot{H}_x - 2C_x\right]\dot{x} = 0$, $\forall \dot{x} \in \mathbb{R}^m$, and actually $\dot{H}_x = C_x + C_x^T$.

Property 10. The dynamic Eq. (3) is linear with respect to its parameters, therefore considering Assumption 2 and Property 3, the gravitational and interaction forces can be rewritten as

$$g_x + f_e = Y_x\theta \tag{5}$$

where $Y_x \in \mathbb{R}^{m\times r}$ is a regression matrix and $\theta \in \mathbb{R}^r$ is a constant vector of parameters associated to gravitational forces and stiffness.

Assumption 3. Because $\tau = J^T(q)f_x$ and according to Property 5 and Assumption 1, each element of f_x is bounded by $\mathcal{F}_j > 0$, i.e., $\left|f_{xj}\right| \leq \mathcal{F}_j$, j = 1, …, m. Assume that

$$f_{xj} = \mathcal{F}_j \mathrm{sat}\left(u_{xj}/\mathcal{F}_j\right) \tag{6}$$

Therefore, $u = J^T(q)u_x$.

3. Adaptive force/position controller

In order to control the robot-environment interaction while respecting the saturation limits of the robotic system, the following adaptive structure is proposed:

$$u_x = -s_P\left(K_P\bar{x}\right) - s_F\left(K_F\bar{f}\right) - s_D\left(K_D\dot{x}\right) + Y_x\hat{\theta} \tag{7}$$

where $\bar{x} = x - x_d$ with $x_d \in \mathbb{R}^m$ being any constant desired position; $\bar{f} = f_e - f_d$ with $f_d \in \mathbb{R}^m$ being any constant desired interaction force; $K_P = \mathrm{diag}\left[k_{P1},...,k_{Pm}\right]$, $K_F = \mathrm{diag}\left[k_{F1},...,k_{Fm}\right]$ and $K_D = \mathrm{diag}\left[k_{D1},...,k_{Dm}\right]$ are positive definite matrices of gain parameters; $s_P(y) = \left(\sigma_{P1}(y_1),..., \sigma_{Pm}(y_m)\right)^T$ and $s_F(y) = \left(\sigma_{F1}(y_1),...,\sigma_{Fm}(y_m)\right)^T$ with $\sigma_{Pj}(\cdot)$ and $\sigma_{Fj}(\cdot)$ being strictly increasing GSFs bounded by M_{Pj} and M_{Fj}, respectively; $s_D(y) = \left(\sigma_{D1}(y_1),...,\sigma_{Dm}(y_m)\right)^T$ with $\sigma_{Dj}(\cdot)$ being GSFs bounded by M_{Dj} and $\left\|s_D\left(K_D\dot{x}\right)\right\| \leq \kappa\left\|\dot{x}\right\|$, $\forall \dot{x} \in \mathbb{R}^m$ with $\kappa > 0$; and $\hat{\theta} \in \mathbb{R}^r$ is the estimated parameter vector obtained from the following auxiliary dynamics

$$\dot{\phi} = -\Gamma Y_x^T\left\{\dot{x} + \epsilon\left[s_P\left(K_P\bar{x}\right) + s_F\left(K_F\bar{f}\right)\right]\right\} \tag{8}$$

$$\hat{\theta} = s_a(\phi) \tag{9}$$

where $\Gamma = \mathrm{diag}\left[\gamma_1,...,\gamma_r\right] \in \mathbb{R}^{r\times r}$ is a constant positive definite diagonal matrix, $\epsilon > 0$ is a constant, $s_a(y) = \left(\sigma_{a1}(y_1),...,\sigma_{ar}(y_r)\right)^T$ with $\sigma_{al}(\cdot)$ being strictly increasing GSFs bounded by M_{al} such that

$$\left|\theta_l\right| < M_{al} \tag{10}$$

$$B_{gi}^{M_a} \triangleq \sum_{l=1}^{p} B_{Gil}M_{al} < T_i \tag{11}$$

where Property 4 and Assumption 1 are considered.

3.1 Closed-loop analysis

Suppose that there exists a constant vector ϕ^* such that $s_a\left(\phi^*\right) = \theta$, or equivalently $\phi_l^* = \sigma_{al}^{-1}\left(\theta_l\right)$, $\forall l \in \{1,..., p\}$. Therefore, from Property 10 we have that $Y_x s_a\left(\phi^*\right) = g_x + f_e$, then by combining the robot model Eq. (3), the environment model Eq. (4) and the control scheme Eqs. (7)-(9), the closed-loop dynamics can be represented as

$$\frac{d}{dt}\begin{bmatrix}\bar{x}\\ \bar{f}\\ \dot{x}\\ \bar{\phi}\end{bmatrix} = \begin{bmatrix}\dot{x}\\ K_e\dot{x}\\ H_x^{-1}\left[-s_P\left(K_P\bar{x}\right) - s_F\left(K_F\bar{f}\right) - s_D\left(K_D\dot{x}\right) + Y_x\bar{s}_a\left(\bar{\phi}\right) - C_x\dot{x} - F_x\dot{x}\right]\\ -\Gamma Y_x^T\left\{\dot{x} + \epsilon\left[s_P\left(K_P\bar{x}\right) + s_F\left(K_F\bar{f}\right)\right]\right\}\end{bmatrix} \tag{12}$$

where $\bar{\phi} = \phi - \phi^*$ represents the vector of parameter estimation error and $\bar{s}_a\left(\bar{\phi}\right) = s_a(\phi) - s_a\left(\phi^*\right) = s_a\left(\bar{\phi} + \phi^*\right) - s_a\left(\phi^*\right)$.

Now, from Eq. (12) under stationary conditions we have that

$$\dot{x} = 0_m \tag{13}$$

$$K_e\dot{x} = 0_m \Leftrightarrow \dot{x} = 0_m \tag{14}$$

$$H_x^{-1}\left[-s_P\left(K_P\bar{x}\right) - s_F\left(K_F\bar{f}\right) + Y_x\bar{s}_a\left(\bar{\phi}\right)\right] = 0_m \tag{15}$$

$$-Y_x^T\left[s_P\left(K_P\bar{x}\right) + s_F\left(K_F\bar{f}\right)\right] = 0_r \tag{16}$$

Therefore, the closed-loop equilibrium vector can be defined

as

$$\begin{bmatrix} \bar{x}_E \\ \bar{f}_E \\ \dot{x}_E \\ \bar{\phi}_E \end{bmatrix} \triangleq \begin{bmatrix} x_E - x_d \\ f_E - f_d \\ 0_m \\ \bar{s}_a\left(\bar{\phi}_E\right) \in ker\left\{Y_{xE}\right\} \end{bmatrix} \tag{17}$$

where $x_E \in \mathbb{R}^m$, $f_E \in \mathbb{R}^m$ and $\bar{\phi}_E \in \mathbb{R}^r$ are the equilibrium vectors of position, force and estimation error, respectively, while $Y_{xE} \in \mathbb{R}^{m \times r}$ denotes the equilibrium regression matrix. Then, the origin is an equilibrium point of the closed-loop system.

3.2 Lyapunov stability analysis

To analyze the stability of the closed-loop equilibrium vector, in the Lyapunov sense, consider the following scalar candidate function

$$\begin{aligned} \mathrm{V}\left(\bar{x},\bar{f},\dot{x},\bar{\phi}\right) &= \frac{1}{2}\dot{x}^T H_x \dot{x} + \int_{0_m}^{\bar{x}} s_P^T\left(K_P z\right) dz + \epsilon \dot{x}^T H_x s_P\left(K_P \bar{x}\right) \\ &+ \int_{0_m}^{\bar{f}} s_F^T\left(K_F z\right) K_e^{-1} dz + \epsilon \dot{x}^T H_x s_F\left(K_F \bar{f}\right) + \int_{0_r}^{\bar{\phi}} \bar{s}_a^T\left(z\right) \Gamma^{-1} dz. \end{aligned} \tag{18}$$

In order to demonstrate that this scalar function is positive definite, we first rewrite Eq. (18) as

$$\begin{aligned} V\left(\bar{x},\bar{f},\dot{x},\bar{\phi}\right) &= \frac{1}{2}\dot{x}^T H_x \dot{x} + \alpha \int_{0_m}^{\bar{x}} s_P^T\left(K_P z\right) dz + \epsilon \dot{x}^T H_x s_P\left(K_P \bar{x}\right) \\ &+ \alpha \int_{0_m}^{\bar{f}} s_F^T\left(K_F z\right) K_e^{-1} dz + \epsilon \dot{x}^T H_x s_F\left(K_F \bar{f}\right) + \int_{0_r}^{\bar{\phi}} \bar{s}_a^T\left(z\right) \Gamma^{-1} dz \\ &+ \left(1-\alpha\right)\left[\int_{0_m}^{\bar{x}} s_P^T\left(K_P z\right) dz + \int_{0_m}^{\bar{f}} s_F^T\left(K_F z\right) K_e^{-1} dz\right] \end{aligned} \tag{19}$$

where $0 < \alpha < 1$. Then, according to Property 6, the following terms of Eq. (19) can be lower bounded by

$$\begin{aligned} &\frac{1}{2}\dot{x}^T H_x \dot{x} \geq \frac{\mu_m}{2}\left\|\dot{x}\right\|^2 \\ &\epsilon \dot{x}^T H_x s_P\left(K_P \bar{x}\right) \geq -\epsilon \mu_M \left\|s_P\left(K_P \bar{x}\right)\right\| \left\|\dot{x}\right\| \\ &\epsilon \dot{x}^T H_x s_F\left(K_F \bar{f}\right) \geq -\epsilon \mu_M \left\|s_F\left(K_F \bar{f}\right)\right\| \left\|\dot{x}\right\| \end{aligned}$$

While using Definitions 1-2 (item 3), we can obtain the lower bounds of the following terms of Eq. (19)

$$\begin{aligned} &\alpha \int_{0_m}^{\bar{x}} s_P^T\left(K_P z\right) dz \geq \frac{\alpha}{2\beta_P}\left\|s_P\left(K_P \bar{x}\right)\right\|^2 \\ &\alpha \int_{0_m}^{\bar{f}} s_F^T\left(K_F z\right) K_e^{-1} dz \geq \frac{\alpha}{2\beta_F}\left\|s_F\left(K_F \bar{f}\right)\right\|^2 \end{aligned}$$

where $\beta_P \triangleq \max_j\left\{\sigma'_{PjM} k_{Pj}\right\}$ and $\beta_F \triangleq \max_j\left\{\sigma'_{FjM} k_{Fj} k_{ej}\right\}$, since

$$\int_{0_m}^{\bar{x}} s_P^T\left(K_P z\right) dz = \sum_{j=1}^{m} \int_0^{\bar{x}_j} \sigma_{Pj}\left(k_{Pj} z_j\right) dz_j$$

and

$$\int_{0_m}^{\bar{f}} s_F^T\left(K_F z\right) K_e^{-1} dz = \sum_{j=1}^{m}\left(1/k_{ej}\right) \int_0^{\bar{f}_j} \sigma_{Fj}\left(k_{Fj} z_j\right) dz_j .$$

Then,

$$\begin{aligned} V\left(\bar{x},\bar{f},\dot{x},\bar{\phi}\right) &\geq \frac{\mu_m}{2}\left\|\dot{x}\right\|^2 + \frac{\alpha}{2\beta_P}\left\|s_P\left(K_P \bar{x}\right)\right\|^2 + \frac{\alpha}{2\beta_F}\left\|s_F\left(K_F \bar{f}\right)\right\|^2 \\ &- \epsilon \mu_M \left\|s_P\left(K_P \bar{x}\right)\right\| \left\|\dot{x}\right\| - \epsilon \mu_M \left\|s_F\left(K_F \bar{f}\right)\right\| \left\|\dot{x}\right\| + \int_{0_r}^{\bar{\phi}} \bar{s}_a^T\left(z\right) \Gamma^{-1} dz \\ &+ \left(1-\alpha\right)\left[\int_{0_m}^{\bar{x}} s_P^T\left(K_P z\right) dz + \int_{0_m}^{\bar{f}} s_F^T\left(K_F z\right) K_e^{-1} dz\right] \end{aligned} \tag{20}$$

Therefore, the scalar function Eq. (18) can be lower bounded by

$$\begin{aligned} V\left(\bar{x},\bar{f},\dot{x},\bar{\phi}\right) &\geq W_1\left(\bar{x},\bar{f},\dot{x}\right) + \int_{0_r}^{\bar{\phi}} \bar{s}_a^T\left(z\right) \Gamma^{-1} dz \\ &+ \left(1-\alpha\right)\left[\int_{0_m}^{\bar{x}} s_P^T\left(K_P z\right) dz + \int_{0_m}^{\bar{f}} s_F^T\left(K_F z\right) K_e^{-1} dz\right] \end{aligned} \tag{21}$$

where

$$W_1\left(\bar{x},\bar{f},\dot{x}\right) = \frac{1}{2}\begin{bmatrix} \left\|s_P\left(K_P \bar{x}\right)\right\| \\ \left\|\dot{x}\right\| \\ \left\|s_F\left(K_F \bar{f}\right)\right\| \end{bmatrix}^T \begin{bmatrix} \dfrac{\alpha}{\beta_P} & -\epsilon\mu_M & 0 \\ -\epsilon\mu_M & \mu_m & -\epsilon\mu_M \\ 0 & -\epsilon\mu_M & \dfrac{\alpha}{\beta_F} \end{bmatrix} \begin{bmatrix} \left\|s_P\left(K_P \bar{x}\right)\right\| \\ \left\|\dot{x}\right\| \\ \left\|s_F\left(K_F \bar{f}\right)\right\| \end{bmatrix} \tag{22}$$

Thus, according to the theorem of Sylvester [28] $W_1\left(\bar{x},\bar{f},\dot{x}\right)$ is a positive definite function if $\alpha/\beta_P > 0$, $\alpha\mu_m/\beta_P > \left[\epsilon\mu_M\right]^2$ and $\alpha\mu_m/\left[\beta_P + \beta_F\right] > \left[\epsilon\mu_M\right]^2$ then we can choose α such that

$$\frac{\epsilon^2}{\epsilon_1^2} < \alpha < 1 \tag{23}$$

where

$$\epsilon_1 \triangleq \sqrt{\mu_m / \left[\mu_M^2\left(\beta_P + \beta_F\right)\right]} \tag{24}$$

Therefore, from inequality Eq. (23) and items 4 and 5 of Definitions 1-2, $V(\bar{x},\bar{f},\dot{x},\bar{\phi})>0$ and radially unbounded.

Now, the upper right-hand derivative of Eq. (18) along the trajectories of the closed-loop system Eq. (12) is

$$\begin{aligned}\dot{V}(\bar{x},\bar{f},\dot{x},\bar{\phi}) &= \frac{1}{2}\dot{x}^T\dot{H}_x\dot{x}+\dot{x}^TH_x\ddot{x}+s_P^T(K_P\bar{x})\dot{\bar{x}}+\epsilon s_P^T(K_P\bar{x})H_x\ddot{x}\\ &\quad+\epsilon\dot{x}^T\dot{H}_xs_P(K_P\bar{x})+\epsilon\dot{x}^TH_xs'_P(K_P\bar{x})K_P\dot{\bar{x}}\\ &\quad+s_F^T(K_F\bar{f})K_e^{-1}\dot{\bar{f}}+\epsilon s_F^T(K_F\bar{f})H_x\ddot{x}+\epsilon\dot{x}^T\dot{H}_xs_F(K_F\bar{f})\\ &\quad+\epsilon\dot{x}^TH_xs'_F(K_F\bar{f})K_F\dot{\bar{f}}+\bar{s}_a^T(\bar{\phi})\Gamma^{-1}\dot{\bar{\phi}}\\ &=-\dot{x}^Ts_D(K_D\dot{x})-\epsilon s_P^T(K_P\bar{x})s_P(K_P\bar{x})-\epsilon s_F^T(K_F\bar{f})s_F(K_F\bar{f})\\ &\quad-2\epsilon s_P^T(K_P\bar{x})s_F(K_F\bar{f})-\epsilon\left[s_P^T(K_P\bar{x})+s_F^T(K_F\bar{f})\right]s_D(K_D\dot{x})\\ &\quad-\epsilon\left[s_P^T(K_P\bar{x})+s_F^T(K_F\bar{f})\right]F_x\dot{x}+\epsilon\dot{x}^TH_xs'_P(K_P\bar{x})K_P\dot{x}\\ &\quad-\epsilon\dot{x}^TC_x\left[s_P(K_P\bar{x})+s_F(K_F\bar{f})\right]+\epsilon\dot{x}^TH_xs'_F(K_F\bar{f})K_FK_e\dot{x}\\ &\quad-\dot{x}^TF_x\dot{x}\end{aligned} \tag{25}$$

where Property 9 was used. Then, by employing Properties 6-8, this function can be upper bounded by

$$\dot{V}(\bar{x},\bar{f},\dot{x},\bar{\phi})\le-\dot{x}^Ts_D(K_D\dot{x})-W_2(\bar{x},\bar{f},\dot{x}) \tag{26}$$

where

$$W_2(\bar{x},\bar{f},\dot{x})=\frac{1}{2}w_2^T\begin{bmatrix}2\epsilon & -\epsilon(f_M+\kappa)\\ -\epsilon(f_M+\kappa) & 2(f_m-\epsilon\beta_M)\end{bmatrix}w_2 \tag{27}$$

with $\beta_M\triangleq k_c\left(\sqrt{\sum_{j=1}^m M_{Pj}^2}+\sqrt{\sum_{j=1}^m M_{Fj}^2}\right)+\mu_M(\beta_P+\beta_F)$ and $w_2=\begin{bmatrix}\left\|s_P(K_P\bar{x})+s_F(K_F\bar{f})\right\|\\ \|\dot{x}\|\end{bmatrix}$.

Thus, by choosing $\epsilon<\epsilon_2$ where

$$\epsilon_2\triangleq 4f_m/\left[4\beta_M+(f_M+\kappa)^2\right]. \tag{28}$$

$W_2(\bar{x},\bar{f},\dot{x})$ is a positive definite function and $\dot{V}(\bar{x},\bar{f},\dot{x},\bar{\phi})\le 0$. Then, the stability of equilibrium vector shall be ensured if

$$\epsilon<\epsilon_M\triangleq\min\{\epsilon_1,\epsilon_2\} \tag{29}$$

and according to LaSalle's invariance principle [25], consider the following set

$$\begin{aligned}\Omega&=\left\{\bar{x},\bar{f},\dot{x}\in\mathbb{R}^m,\bar{\phi}\in\mathbb{R}^r:\dot{V}(\bar{x},\bar{f},\dot{x},\bar{\phi})=0\right\}\\ &=\left\{\bar{x}=\bar{f}=\dot{x}=0_m,\bar{\phi}\in\mathbb{R}^r\right\}\end{aligned} \tag{30}$$

Thus, $\bar{x}=\bar{f}=\dot{x}=0_m\Rightarrow\dot{\bar{f}}=\ddot{x}=0_m$ and from the closed-loop dynamics Eq. (12), $Y_{xE}\bar{s}_a(\bar{\phi}_E)=0_m$. Therefore, the closed-loop equilibrium vector is asymptotically stable.

3.3 Boundedness analysis

The adaptive force/position controller Eqs. (7)-(9) ensures that the generated torques are inside the limits of robot actuators. First, in robot-environment interaction tasks, the deformation of environment is bounded and there are positive constants B_{ej} such that $|x_j-x_{ej}|\le B_{ej}$, j = 1, …, m. Then, we are assuming that strictly increasing LGSFs can reproduce the force-deformation relationship before fracture and the following assumption turns out to be crucial.

Assumption 4. A bounded version of model Eq. (4) can be represented by

$$f_e=K_es_e(x-x_e) \tag{31}$$

where $s_e(y)=(\sigma_{e1}(y_1),...,\sigma_{em}(y_m))^T$ with $\sigma_{ej}(\cdot)$ being strictly increasing LGSFs bounded by M_{ej}. Thus, the vector of parameters θ can be represented as

$$\theta=\begin{bmatrix}\theta_g\\ \theta_e\end{bmatrix} \tag{32}$$

where $\theta_e\in\mathbb{R}^m$ is a constant vector which depends on the stiffness of environment, then $r=p+m$ and

$$Y_x\theta=G_x\theta_g+F_e\theta_e \tag{33}$$

where $G_x=\left[J^{-1}(q)\right]^TG(q)\in\mathbb{R}^{m\times p}$ (see Property 3) and $F_e=\mathrm{diag}\left[\sigma_{e1}(x_1-x_{e1}),...,\sigma_{em}(x_m-x_{em})\right]\in\mathbb{R}^{m\times m}$ are regression matrices.

Now, by considering Assumption 4, the controller Eq. (7) can be rewritten as $u_x=u_{PFD}+G_x\hat{\theta}_g$ where

$$u_{PFD}=-s_P(K_P\bar{x})-s_F(K_F\bar{f})-s_D(K_D\dot{x})+F_e\hat{\theta}_e \tag{34}$$

Then, in order to avoid the actuator saturation, we have that

$$|u_i|=\left|J_i^T(q)u_x\right|=\left|J_i^T(q)u_{PFD}+G_i(q)\hat{\theta}_g\right|<T_i \tag{35}$$

and according to Eq. (9) and Property 4, there are non-negative constants $B_{gi}^{M_a}$ such that

$$\left|G_i(q)\hat{\theta}_g\right|\le B_{gi}^{M_a} \tag{36}$$

$i=1,\ldots,n$; and now Eq. (35) can be rewritten as

$$\left|J_i^T(q)u_{PFD}\right|\le\left\|J_i^T(q)\right\|\left\|u_{PFD}\right\|<T_i-B_{gi}^{M_a} \tag{37}$$

Therefore, from Property 5, the following sufficient condition to avoid actuator saturation can be set

$$\sqrt{\sum_{j=1}^{m}\left[M_{Pj}+M_{Fj}+M_{Dj}+M_{a(p+j)}M_{ej}\right]^2}<u_M \tag{38}$$

where

$$u_M \triangleq \min_i\left\{\frac{T_i-B_{gi}^{M_a}}{B_{Ji}}\right\} \tag{39}$$

However, being Eq. (38) a condition only sufficient and not necessary, successful results avoiding saturation can be obtained with values of $\left[T_i-B_{gi}^{M_a}\right]/B_{Ji}$ greater than u_M.

4. Numerical simulation

In order to evaluate the performance of the proposed control scheme, an interaction task was implemented in MATLAB® R2020b using the model of an anthropomorphic robot manipulator of 3 degrees of freedom. The nominal parameters of this robot manipulator were reported in Ref. [30]; whose maximum joint torques are T_1 = 50 Nm, T_2 = 150 Nm and T_3 = 15 Nm, respectively; and the positive constants that satisfy Properties 5 to 8 are B_{J1} = 0.93, B_{J2} = 0.9, B_{J3} = 0.45, μ_m = 0.531, μ_M = 3589, k_c = 39925, f_m = 0.722 and f_M = 3295, respectively. The nominal parameters associated with gravity are θ = [55.628, 0.273, 1.996, 0.696]^T Nm.

In addition, to address some practical issues, position, speed and force measurements were considered to contain additive white noise, taking into account the information provided by the manufacturers of the sensors of robot used in Refs. [14, 30]. First, in the case of angular position measurement, an error of 1 incremental-encoder pulse corresponding to 6.136×10^{-6} rad was considered. While the angular velocity was computed by a dirty derivative with a sampling period of 2.5 ms. Finally, for the force sensor, the transducer was considered to have a 1.5 % error.

4.1 Description of the interaction task

The robot manipulator must perform a point interaction on a flat and rigid surface as shown in Fig. 1. In order to simplify the planning of interaction task, it was represented with respect to the coordinated frame (x_p, y_p, z_p) attached to the environment (surface) and which in industrial robotics is called user frame. The origin of user reference frame is located at (0.5, 0.35, -0.49) m and the surface is an inclined plane at 30 degrees from the horizontal with a stiffness value normal to the plane of 2000 N/m, therefore K_e = diag {0, 1000, 1732.05} N/m. Without loss of generality, it is assumed that only non-zero interaction forces need to be compensated and, therefore, the control scheme will only be adapted to non-zero stiffness components. Then, assume that the position of the robot's end

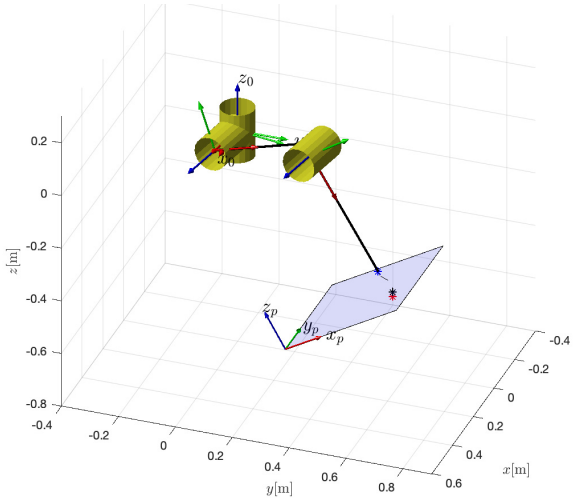

Fig. 1. Graphical representation of the interaction task, where the system (x_p, y_p, z_p) represents the coordinate frame attached to the plane (user frame) and (x_0, y_0, z_0) is the reference frame at the origin of the robot.

effector with respect to the user frame is

$$\begin{bmatrix} x_{pe1} \\ x_{pe2} \\ x_{pe3} \\ 1 \end{bmatrix} = H_e^{-1}\begin{bmatrix} x_1 \\ x_2 \\ x_3 \\ 1 \end{bmatrix} \tag{40}$$

where H_e is the following homogeneous transformation matrix

$$H_e = \begin{bmatrix} 0 & -1 & 0 & 0.5 \\ 0.866 & 0 & -0.5 & 0.35 \\ 0.5 & 0 & 0.866 & -0.49 \\ 0 & 0 & 0 & 1 \end{bmatrix} \tag{41}$$

The robot starts the movement from the initial configuration $q(0)$ = [-10, 110, -75]^T degrees or equivalently $x(0)$ = (0.364, 0.627, -0.215) m and must reach the desired position x_d = (0.307, 0.658, -0.335) m, however the surface does not allow it and during contact the robot must interact with the environment by applying a force f_d = [0, -5, 8.66]^T N (which is equivalent to a normal force of 10 N).

4.2 Configuration of the adaptive force/position controller

For the implementation of the controller Eqs. (7)-(9) the following generalized saturation functions were used

$$\sigma_h(\varsigma;M) = M\ \text{sat}(\varsigma/M) \tag{42}$$

$$\sigma_s(\varsigma;L,M) = \begin{cases} \varsigma, & \forall|\varsigma|\le L \\ \rho_s(\varsigma), & \forall|\varsigma|>L \end{cases} \tag{43}$$

where

$$\rho_s(\varsigma)=\operatorname{sign}(\varsigma)L+(M-L)\tanh\left(\frac{\varsigma-\operatorname{sign}(\varsigma)L}{M-L}\right) \tag{44}$$

Then, the proportional actions of position and force, as well as the derivative action and the adaptive term were implemented with

$$\sigma_{Pj}(\varsigma)=\sigma_s(\varsigma;L_{Pj},M_{Pj}) \tag{45}$$

$$\sigma_{Fj}(\varsigma)=\sigma_s(\varsigma;L_{Fj},M_{Fj}) \tag{46}$$

$$\sigma_{Dj}(\varsigma)=\sigma_h(\varsigma;M_{Dj}) \tag{47}$$

$$\sigma_{al}(\varsigma)=\sigma_s(\varsigma;L_{al},M_{al}) \tag{48}$$

j = 1, 2, 3 and l = 1, 2, …, 7. Therefore, $\sigma'_{PjM}=\sigma'_{FjM}=\sigma'_{DjM}=\sigma'_{al}=1$ and $\kappa=\max_j\{k_{Dj}\}$. While the regression matrix is given by

$$Y_x=\begin{bmatrix} G_{x11} & G_{x12} & G_{x13} & G_{x14} & F_{e11} & 0 & 0\\ G_{x21} & G_{x22} & G_{x23} & G_{x24} & 0 & F_{e22} & 0\\ G_{x31} & G_{x32} & G_{x33} & G_{x34} & 0 & 0 & F_{e33}\end{bmatrix} \tag{49}$$

where

$$G_{x11}=\delta_1\sin q_2\sin(q_2+q_3)$$
$$G_{x12}=\delta_1\cos q_2\sin(q_2+q_3)$$
$$G_{x13}=-\delta_1\sin q_2\sin(q_2+q_3)$$
$$G_{x14}=-\delta_1\sin q_2\cos(q_2+q_3)$$
$$G_{x21}=\delta_2\sin q_2\sin(q_2+q_3)$$
$$G_{x22}=\delta_2\cos q_2\sin(q_2+q_3)$$
$$G_{x23}=-\delta_2\sin q_2\sin(q_2+q_3)$$
$$G_{x24}=-\delta_2\sin q_2\cos(q_2+q_3)$$
$$G_{x31}=\delta_3\sin q_2\cos(q_2+q_3)$$
$$G_{x32}=\delta_3\cos q_2\cos(q_2+q_3)$$
$$G_{x33}=-\delta_3\cos q_2\sin(q_2+q_3)$$
$$G_{x34}=-\delta_3\cos q_2\cos(q_2+q_3)$$
$$F_{e11}=0$$
$$F_{e22}=\begin{cases}0, & \forall x_{pe3}\ge 0\\ -\sigma_{e2}(x_{pe3}), & \forall x_{pe3}<0\end{cases}$$
$$F_{e33}=\begin{cases}0, & \forall x_{pe3}\ge 0\\ \sigma_{e3}(x_{pe3}), & \forall x_{pe3}<0\end{cases}$$

with

$$\delta_1=\frac{1}{a\sin q_3}\left[\frac{d\cos q_1}{a\left[\sin q_2+\sin(q_2+q_3)\right]}-\sin q_1\right]$$

$$\delta_2=\frac{1}{a\sin q_3}\left[\frac{d\sin q_1}{a\left[\sin q_2+\sin(q_2+q_3)\right]}+\cos q_1\right]$$

$$\delta_3=-\frac{1}{a\sin q_3}$$

$$\sigma_{ej}(\varsigma)=\sigma_s(\varsigma;L_{ej},M_{ej})$$

j = 2, 3; a = 0.45 m and d = 0.25 m. Then, $M_{el}=M_{a5}=0$ and the number of parameters associated with gravity are p = 4.

4.3 Results

To properly perform the robot-environment interaction task described above, the parameters of controller Eqs. (7)-(9) were selected according to the following procedure:

1. Set the parameters M_{al} and L_{al} satisfying inequality Eq. (10) and compute the constants $B_{gi}^{M_a}$ using Eq. (11).
2. Set the parameters M_{ej} and L_{ej} according to the maximum deformation values expected during the interaction task.
3. Set the parameters M_{Dj}, M_{Pj}, L_{Pj}, M_{Fj} and L_{Fj} satisfying inequality Eq. (38) and trying to respect the condition Eq. (39), if possible, or increasing the value of u_M as far as the maximum torque values permit it.
4. Run simulations/experiments with low control gains (k_{Dj}, k_{Pj}, k_{Fj}, γ_l).
5. Increase the proportional gains, (k_{Pj}, k_{Fj}), to reduce the rise time (speed up the closed-loop response).
6. Increase the derivative gains, k_{Dj}, to reduce inertial effects, such as the overshoot.
7. Increase the adaptive gains, γ_l, to strengthen the elimination of position and force errors, by reducing stabilization times (speed up the parameter convergence).
8. Adjust ϵ satisfying inequality Eq. (29), if possible, or increasing its value as far as the closed-loop stability permits it.
9. Repeat steps 5-8 until the best possible response is obtained.

Therefore, the selected parameters are presented in Table 1 and the corresponding results are shown in Figs. 2-6, where the subscript n corresponds to signals containing additive white noise. To implement the adaptive term, we chose as an initial condition $\hat{\theta}$ = [51, 0.1, 1.2, 0.4, 0, 1500, 2200]^T. Fig. 2 shows the position errors ($\bar{x}_1$, $\bar{x}_2$, $\bar{x}_3$) corresponding to the x, y and z components, respectively. We can observe that all components tend to zero before there is contact with the environment; however, in particular for the z component a steady-state error is observed because of the contact with the surface, which is a desired feature according to the closed-loop equilibrium vector Eq. (17). Therefore, the robot end effector remains on the surface of environment without damaging it and regulating the contact force as seen in Fig. 3, which is described below. It is also important to note that the noise present in the angular position measurements only slightly affects the transient response and yet the control objective is still met.

A very important feature of explicit force control schemes is

Table 1. Tuning of controller parameters.

Parameter	Value
$(M_{a1}, M_{a2}, M_{a3}, M_{a4}, M_{a5}, M_{a6}, M_{a7})$	(58, 1, 3, 1, 0, 2400, 2400)
L_{al}	$0.9M_{al}$, l = 1, 2, …, 7
(M_{e1}, M_{e2}, M_{e3})	(0, 0.005, 0.005)
L_{ej}	$0.7M_{ej}$, j = 1, 2, 3
u_M	96.6666
(M_{p1}, M_{p2}, M_{p3})	(15, 10.2, 25)
L_{pj}	$0.9M_{pj}$, j = 1, 2, 3
(M_{F1}, M_{F2}, M_{F3})	(5, 8, 20)
L_{Fj}	$0.9M_{Fj}$, j = 1, 2, 3
(M_{D1}, M_{D2}, M_{D3})	(3, 5, 30)
K_P	diag{650, 700, 40}
K_F	diag{3500,800, 1560}
K_D	diag{1000, 150, 92}
Γ	diag{25, 3.5, 24.5, 6, 1, 5.4×10^7, 5.2×10^7}
ϵ	5.8×10^{-11}

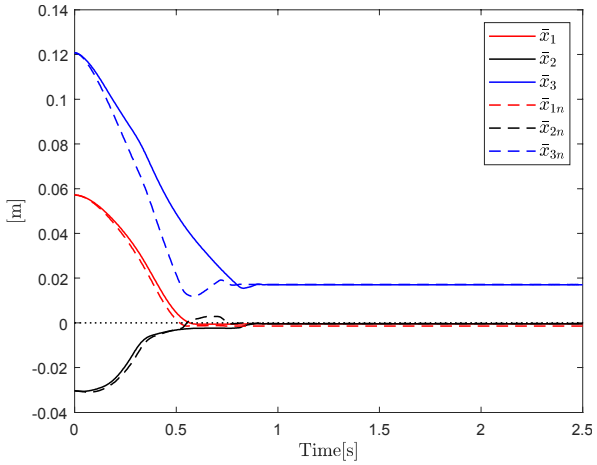

Fig. 2. Position errors obtained when using the proposed controller.

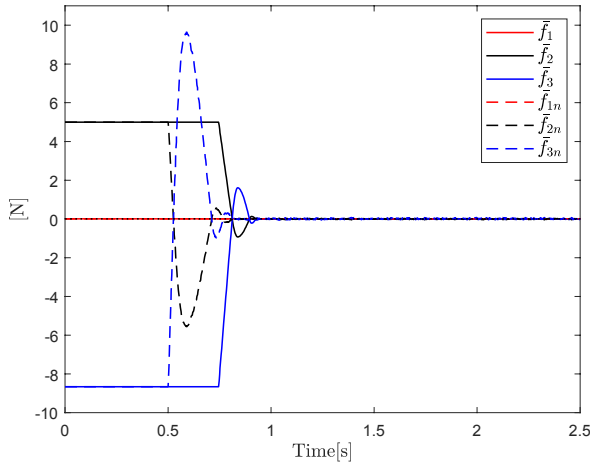

Fig. 3. Force errors obtained when using the proposed controller.

that they can regulate the contact force during robot-environment interaction, and this is accomplished appropriately with the proposed controller as can be seen in Fig. 3, where all the components of force error tend to zero despite the presence of additive white noise in the force measurements, as again only the transient response is affected.

One property of the proposed control scheme is that, in the presence of parametric uncertainty, it can compensate for this uncertainty by adapting to the effects generated by gravitational and contact forces. In Figs. 4 and 5, we can see that both the parameters associated with gravitational torques and the stiffness components of environment are properly estimated in less than 1 second, for the noise-free case, according to the nominal values presented above. On the other hand, when there is noise in the measurements, the evolution of all parameters remains bounded and this is again consistent with the stability analysis. If we want to improve the convergence of parameters, we can adjust the gains in matrix Γ.

Moreover, the most important advantage of the proposed control scheme over the previously presented controllers is that our force/position regulator ensures that the control torques

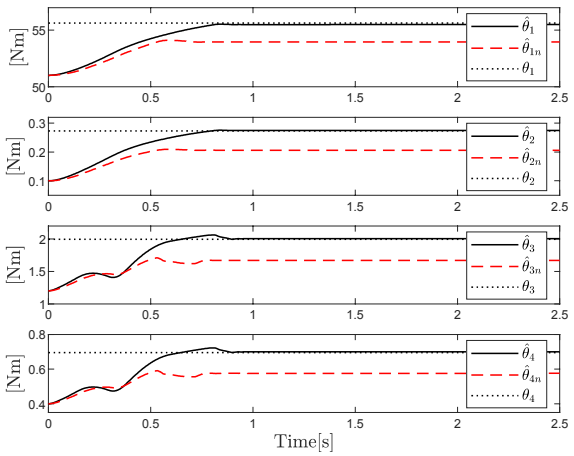

Fig. 4. Estimation of parameters associated with gravity.

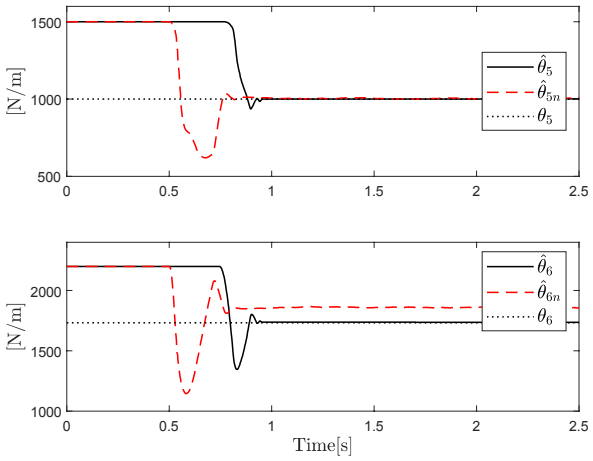

Fig. 5. Estimation of parameters associated with stiffness.

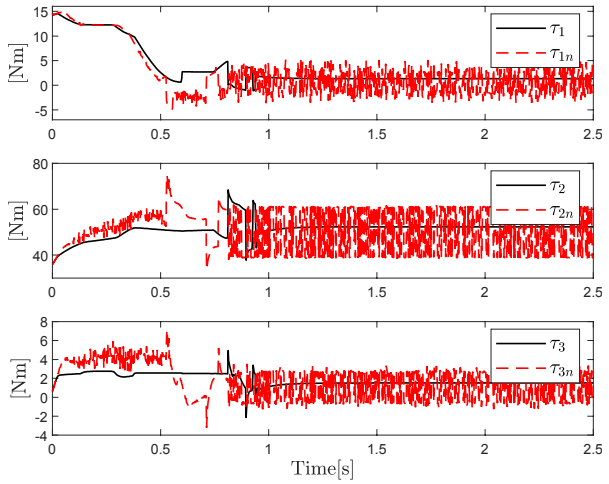

Fig. 6. Control torques obtained when using the proposed controller.

remain bounded all the time. The torques applied to the robot are presented in Fig. 6 and it can be observed that all three remain below the torque limits of robot actuators defined previously. However, in this case, the effect of noise on the measurements is more evident, since the calculation of velocities by dirty derivative causes the noise to be amplified and again, we must make an adjustment of the controller gains to minimize it.

Finally, in order to compare our results with a recent force/position control scheme, we selected the controller presented in Ref. [17] and given by

$$x_r = x_d - K_{Pf}\bar{f} - K_{If}\int_0^t \bar{f}(z)\,dz \tag{50}$$

where $x_r \in \mathbb{R}^m$ represents the reference position, which must be transformed to joint coordinates using the robot's inverse kinematics to get the joint position error $\bar{q} = q - q_r \in \mathbb{R}^n$ and then processed by a traditional PID controller. The gain parameters of controller Eq. (50) were selected as K_{Pf} = 1×10^{-3}diag{1, 1, 1} and K_{If} = 1×10^{-3}diag{10, 10, 12} to obtain the best possible response, since the authors do not suggest a tuning process in Ref. [17].

Figs. 7-9 show the results obtained with the controller proposed in Ref. [17]. In particular, Fig. 7 shows that there is no zero convergence of the position error components even though the controller includes an integral action. While all force errors converge to zero as seen in Fig. 8, thanks to the fact that the structure of the controller includes two nested integral actions for force regulation. In addition, again the additive white noise mainly modifies transient state behavior, although in this case more significant overshoots are obtained because a softened force reference was not used as in Ref. [17]. This is another advantage of our proposal, as the use of GSFs allows to minimize overshoots.

In Fig. 9, the control torques of the scheme proposed in Ref. [17] are presented and it can be seen that the inclusion of integral actions minimizes the effect of noise, however, the limit

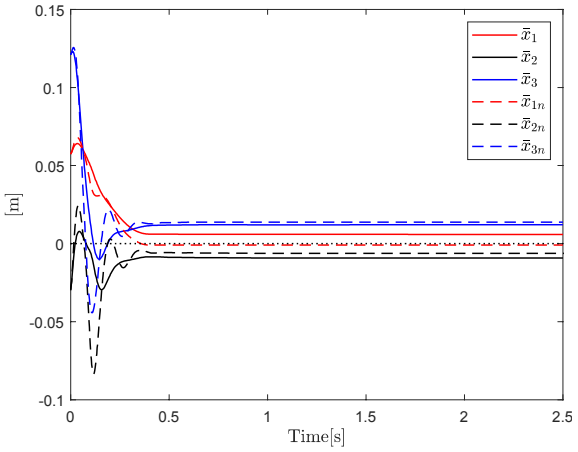

Fig. 7. Position errors obtained when using the controller proposed in Ref. [17].

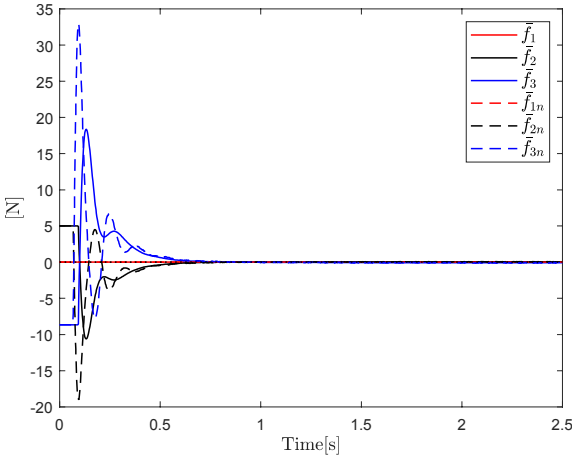

Fig. 8. Force errors obtained when using the controller proposed in Ref. [17].

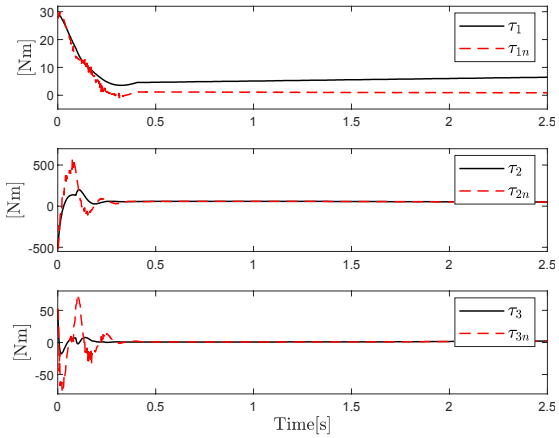

Fig. 9. Control torques obtained when using the controller proposed in Ref. [17].

torques T_2 = 150 Nm and T_3 = 15 Nm are exceeded during the transient stage. This is because the control structure does not guarantee the generation of bounded actions as our pro-

Table 2. Performance indices for the noise-free test and the white-noise (WN) one.

Index	Our controller	Controller of Ref. [17]
$\mathcal{L}_2$ -norm of position error (TS)	0.075 m 0.068 m (WN)	0.039 m 0.042 m (WN)
$\mathcal{L}_2$ -norm of position error (SS)	0.022 m 0.022 m (WN)	0.021 m 0.020 m (WN)
$\mathcal{L}_2$ -norm of force error (TS)	8.759 N 7.866 N (WN)	5.839 N 7.489 N (WN)
$\mathcal{L}_2$ -norm of force error (SS)	0.002 N 0.071 N (WN)	0.083 N 0.102 N (WN)
$\mathcal{L}_\infty$ -norm of control torque 1	14.59 Nm 14.86 Nm (WN)	28.63 Nm 29.75 Nm (WN)
$\mathcal{L}_\infty$ -norm of control torque 2	68.43 Nm 74.89 Nm (WN)	518.57 Nm 591.31 Nm (WN)
$\mathcal{L}_\infty$ -norm of control torque 3	4.94 Nm 7.15 Nm (WN)	51.65 Nm 78.35 Nm (WN)

posal does. On the other hand, from these results, it is observed that the price to pay for our scheme to generate bounded actions are longer transient states.

Finally, in order to carry out a quantitative evaluation of the performance of both controllers, the following indices were considered:

1. $\mathcal{L}_2$ -norm, defined as

$$\|e\|_{\mathcal{L}_2} = \sqrt{\frac{1}{t-t_0}\int_{t_0}^{t} e^T(z)e(z)dz}$$

where $e \in \mathbb{R}^m$ represents the position or force error.

2. $\mathcal{L}_\infty$ -norm, defined as

$$\|\tau_i\|_{\mathcal{L}_\infty} = \max_t \{|\tau_i(t)|\}$$

where $i = 1, \ldots, n$.

The performance indices obtained for each controller are presented in Table 2. The error norms were calculated for both the transient state (TS) and the steady state (SS), considering a settling time of 1 second, and the following can be concluded: 1) The kinematic controller [17] has a better performance with respect to the error in the transient state, because it has a faster response but at the cost of requesting torques outside the limits allowed by the actuators and this could compromise its performance in experimental tests; 2) The steady state performance of the two controllers with respect to position error is very similar, therefore, with proper tuning of gains good results are obtained in both cases; 3) The force error norm in the steady state is smaller for our controller, therefore, our is scheme has better force regulation and this is because the controller [17] is kinematic and does not directly regulate force; 4) The maximum torques requested by our controller are lower and within the limits of the actuators, thus ensuring greater safety for the robot and its environment.

5. Conclusions

In this paper, an adaptive approach to force/position control has been presented that guarantees the generation of bounded control actions. Therefore, our proposal addresses the problem of explicit force control by ensuring the non-saturation of robot actuators, without limiting the tuning of gains to improve performance, thanks to the use of generalized saturation functions and it is supported by a rigorous stability analysis in the Lyapunov sense. In addition, the control scheme is robust in the presence of parametric uncertainty, and this allows to compensate for external forces generated by gravitational effects and robot-environment interaction. Furthermore, good results were obtained in numerical simulation that are quite reliable as an academic example that supports our theoretical development, since the performance obtained is comparable with the state-of-the-art schemes but with the advantage of generating bounded actions. Therefore, this type of control scheme has as potential applications industrial tasks of polishing or machining, as well as the force regulation of medical robots such as prosthetics, exoskeletons and rehabilitation, assistance, or surgery systems.

As future work, we will further investigate how to improve the performance of this type of controllers by focusing on the following aspects: a) minimize the effect of noise in practice by including integral actions within the structure of the controller, b) develop force/position control schemes that operate in the articular space and thus avoid the use of the robot's Jacobian that limits the stability region of closed-loop equilibrium point, c) improve the performance of myoelectric prostheses by using these types of explicit force controllers with bounded actions.

Acknowledgments

This work was supported by the National Council for Science and Technology (grant 2018-000012-01NACF-11014), Mexico, and the Autonomous University of Aguascalientes (PII19-2).

References

[1] M. Roozegar, M. J. Mahjoob and M. Ayati, Adaptive tracking control of a nonholonomic pendulum-driven spherical robot by using a model-reference adaptive system, *Journal of Mechanical Science and Technology*, 32 (2) (2018) 845-853.

[2] H. Seo and S. Lee, Design of general-purpose assistive exoskeleton robot controller for upper limbs, *Journal of Mechanical Science and Technology*, 33 (7) (2019) 3509-3519.

[3] A. Pervez and J. Ryu, Safe physical human robot interaction-past, present and future, *Journal of Mechanical Science and Technology*, 22 (3) (2008) 469-483.

[4] B. Yao, Z. Zhou, L. Wang, W. Xu and Q. Liu, Sensor-less external force detection for industrial manipulators to facilitate physical human-robot interaction, *Journal of Mechanical Science and Technology*, 32 (10) (2018) 4909-4923.

[5] J. H. Kim, H. S. Yoon, H. Moon, H. R. Choi and J. C. Koo, Application of a sensor fusion algorithm for improving grasping

stability, *Journal of Mechanical Science and Technology*, 29 (7) (2015) 2693-2698.
[6] E. Kilic, EMG based neural network and admittance control of an active wrist orthosis, *Journal of Mechanical Science and Technology*, 31 (12) (2017) 6093-6106.
[7] R. Arora and T. K. Bera, Impedance control of three dimensional hybrid manipulator, *Journal of Mechanical Science and Technology*, 34 (1) (2020) 359-367.
[8] A. Winkler and J. Suchý, Explicit and implicit force control of an industrial manipulator-an experimental summary, *Proc. of the 21st IEEE International Conference on Methods and Models in Automation and Robotics*, Miedzyzdroje, Poland (2016) 19-24.
[9] A. Del Prete, F. Nori, G. Metta and L. Natale, Prioritized motion-force control of constrained fully-actuated robots: task space inverse dynamics, *Robotics and Autonomous Systems*, 63 (1) (2015) 150-157.
[10] M. E. Karar, A simulation study of adaptive force controller for medical robotic liver ultrasound guidance, *Arabian Journal for Science and Engineering*, 43 (8) (2018) 4229-4238.
[11] E. Arefinia, H. A. Talebi and A. Doustmohammadi, A robust adaptive model reference impedance control of a robotic manipulator with actuator saturation, *IEEE Transactions on Systems, Man, and Cybernetics: Systems*, 50 (2) (2017) 409-420.
[12] L. Roveda, F. Vicentini and L. M. Tosatti, Deformation-tracking impedance control in interaction with uncertain environments, *Proc. of IEEE/RSJ International Conference on Intelligent Robots and Systems*, Tokyo, Japan (2013) 1992-1997.
[13] A. Azizi, Applications of artificial intelligence techniques to enhance sustainability of industry 4.0: design of an artificial neural network model as dynamic behavior optimizer of robotic arms, *Complexity* (2020) 1-10.
[14] C. Chávez-Olivares, F. Reyes-Cortés and E. González-Galván, On explicit force regulation with active velocity damping for robot manipulators, *Automatika,* 56 (4) (2015) 478-490.
[15] A. Winkler and J. Suchý, Implicit force control of a position controlled robot-a comparison with explicit algorithms, *International Journal of Computer and Information Engineering*, 9 (6) (2015) 1447-1453.
[16] M. Rani and N. Kumar, A new hybrid position/force control scheme for coordinated multiple mobile manipulators, *Arabian Journal for Science and Engineering*, 44 (3) (2019) 2399-2411.
[17] A. Gutierrez-Giles, L. U. Evangelista-Hernandez, M. Arteaga, C. A. Cruz-Villar and A. Rodriguez-Angeles, A force/motion control approach based on trajectory planning for industrial robots with closed control architecture, *IEEE Access*, 9 (2021) 80728-80740.
[18] D. Huang, H. Zhan and C. Yang, Impedance model-based optimal regulation on force and position of bimanual robots to hold an object, *Complexity* (2020) 1-13.
[19] A. Zavala-Rio, M. Mendoza, V. Santibáñez and F. Reyes, Output-feedback proportional-integral-derivative-type control with multiple saturating structure for the global stabilization of robot manipulators with bounded inputs, *International Journal of Advanced Robotic Systems*, 13 (5) (2016).
[20] D. J. López-Araujo, A. Zavala-Río, V. Santibáñez and F. Reyes, A generalized global adaptive tracking control scheme for robot manipulators with bounded inputs, *International Journal of Adaptive Control and Signal Processing*, 29 (2) (2015) 180-200.
[21] G. I. Zamora-Gómez, A. Zavala-Río, D. J. López-Araujo, E. Nuño and E. Cruz-Zavala, Further advancements on the output-feedback global continuous control for the finite-time and exponential stabilisation of bounded-input mechanical systems: desired conservative-force compensation and experiments, *International Journal of Control*, 93 (7) (2020) 1521-1533.
[22] G. I. Zamora-Gómez, A. Zavala-Río, D. J. López-Araujo, E. Cruz-Zavala and E. Nuño, Continuous control for fully damped mechanical systems with input constraints: finite-time and exponential tracking, *IEEE Transactions on Automatic Control*, 65 (2) (2019) 882-889.
[23] M. Rodríguez-Liñán, M. Mendoza, I. Bonilla and C. Chávez-Olivares, Saturating stiffness control of robot manipulators with bounded inputs, *International Journal of Applied Mathematics and Computer Science*, 27 (1) (2017) 79-90.
[24] C. Vidrios-Serrano, M. Mendoza, I. Bonilla and B. Maldonado-Fregoso, A generalized vision-based stiffness controller for robot manipulators with bounded inputs, *International Journal of Control, Automation and Systems*, 19 (1) (2021) 548-561.
[25] J. Pliego-Jiménez, M. Arteaga-Pérez and P. Sánchez-Sánchez, Dexterous robotic manipulation via a dynamic sliding mode force/position control with bounded inputs, *IET Control Theory and Applications*, 13 (6) (2019) 832-840.
[26] T. Ohhira, K. Yokota, S. Tatsumi and T. Murakami, A robust hybrid position/force control considering motor torque saturation, *IEEE Access*, 9 (2021) 34515-34528.
[27] H. K. Khalil, *Nonlinear Systems*, 3rd Ed., Prentice Hall, Upper Saddle River, NJ, USA (2002).
[28] R. Kelly, V. Santibáñez and J. A. Loría, *Control of Robot Manipulators in Joint Space*, Springer Science & Business Media, Leipzig, Germany (2006).
[29] C. Canudas, B. Siciliano and G. Bastin (Eds), *Theory of Robot Control*, Springer Science and Business Media, London, UK (2012).
[30] C. Chávez-Olivares, F. Reyes-Cortés, E. González-Galván, M. Mendoza and I. Bonilla, Experimental evaluation of parameter identification schemes on an anthropomorphic direct drive robot, *International Journal of Advanced Robotic Systems*, 9 (5) (2012).

Lina Rojas-García received the B.E. degree in electronics engineering from the Technology Institute of San Luis Potosi, Mexico, in 2006, the M.Eng. degree in electrical engineering from the Autonomous University of San Luis Potosi, Mexico, in 2012. She is currently pursuing a Ph.D. degree in engineering sciences at the Autonomous University of San Luis Potosi, Mexico. Her current research interests include prosthetic robot control.

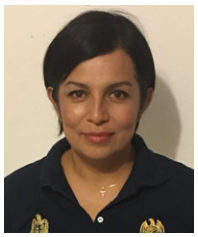

Isela Bonilla-Gutiérrez received the B.E. degree in communications and electronics from the University of Colima, Mexico, in 2003, the M.Sc. degree in electronics from the Autonomous University of Puebla, Mexico, in 2006, and the Ph.D. degree in electrical engineering from the Autonomous University of San Luis Potosi, in 2011. She is currently Full Professor of electronics at the Faculty of Science, Autonomous University of San Luis Potosi, Mexico. Her research interests include robot control and rehabilitation robotics.

Marco Mendoza-Gutiérrez received the B.E. degree in communications and electronics from the University of Colima, Mexico, in 2003, the M.Sc. degree in electronics from the Autonomous University of Puebla, Mexico, in 2006, and the Ph.D. degree in electrical engineering from the Autonomous University of San Luis Potosi, Mexico, in 2011. He is currently Full Professor of biomedical engineering at the Faculty of Science, Autonomous University of San Luis Potosi, Mexico. His research interests include robot control and biorobotics.

César Chávez-Olivares received the B.E. degree in electronics engineering from the Autonomous University of Aguascalientes, Mexico, in 2006, and the MEng and Ph.D. degrees in electrical engineering from the Autonomous University of San Luis Potosi, Mexico, in 2009 and 2014, respectively. He joined the Center of Engineering Sciences at the Autonomous University of Aguascalientes, in 2015, where he is currently professor of robotics engineering. His research interests include biorobotics, haptic devices, identification and control of robot manipulators.